Available online at www.sciencedirect.com

SciVerse ScienceDirect

Scripta Materialia 67 (2012) 826–829

Scripta MATERIALIA

www.elsevier.com/locate/scriptamat

# Fabrication of tungsten carbide–vanadium carbide core–shell structure powders and their application as an inhibitor for the sintering of cemented carbides

Nan Lin,[a] Yuehui He,[a,*] Chonghu Wu,[b,*] Qiankun Zhang,[a] Jin Zou[c] and Zhongwei Zhao[a,d]

[a]*State Key Laboratory for Powder Metallurgy, Central South University, Changsha 410083, People's Republic of China*
[b]*China National R&D Center for Tungsten Technology, Xiamen Tungsten Co. Ltd. Technology Center, Xiamen 361009, People's Republic of China*
[c]*School of Mechanical and Mining Engineering, Centre for Microscopy and Microanalysis, The University of Queensland, Brisbane, QLD 4072, Australia*
[d]*School of Metallurgical Science and Engineering, Central South University, Changsha, People's Republic of China*

Received 25 April 2012; accepted 30 July 2012
Available online 4 August 2012

---

An innovative way to synthesize tungsten carbide–vanadium carbide core–shell structure powders, which are predicted to act as inhibitors for cemented carbides, has been explored. The core–shell structures were synthesized by chemically induced precipitation and carbonization reactions. The cemented carbides with a homogeneous microstructure were prepared at 1400 °C. The existence of tungsten carbide–vanadium carbide core–shell structure can significantly refine tungsten carbide grains, inhibit the abnormal growth of finer grains in the liquid sintering and improve the mechanical properties of the hard metals.

*Keywords:* Nanocomposite; Transmission electron microscopy; Cermets; Hardness; Ultrafine-grained microstructure

---

Owing to their high hardness, wear resistance and excellent fracture resistance, cemented tungsten carbides are widely applied in the metal machining, drilling and mining industries [1–4]. Tungsten carbides are typically composed of a metal ceramic and a cobalt binder. Refining the grain size of tungsten carbides significantly improves the mechanical properties of cemented tungsten carbides [5,6]. Initial ultrafine WC powders can been prepared by various methods, such as mechanical ball-milling, spray conversion, and chemical vapor phase reaction synthesis, etc. [7–10]. However, a significantly finer WC grain growth inevitably occurs when sintering WC–Co powder mixtures by a conventional liquid-state sintering process. The most effective ways of controlling the finer WC grain growth during the sintering process have usually depended on the addition of some WC grain growth inhibitors such as VC, $Cr_3C_2$ and TaC, incorporated by mechanical mixing, of which VC is the most effective inhibitor. However, it is difficult to disperse a small amount of inhibitor powder uniformly within the initial mixed powders by ball milling [11]. During conventional liquid-phase sintering, the dissolution of VC in the binder phase suppresses the solution–reprecipitation of tungsten carbides which causes the grain growth of WC particles during the sintering of WC–Co materials [2]. The nonuniformity of inhibitors results in non-homogeneous WC solubility in the binder phase, which causes abnormal grain growth and results finally in the non-homogeneous distribution of WC grain size in the cemented carbides. The defects inevitably damage the mechanical properties of the cemented carbides.

Herein we present a facile process to prepare WC–VC core–shell structure powders. Essentially, the $WO_3$–$V_2O_5$ precursor nanopowders with a designed core–shell structure have been fabricated via a calcination process of the composite salt synthesized by a chemically induced precipitation. In the process, the thickness of

---

* Corresponding authors. Tel.: +86 0731 88836144; fax: +86 0731 88710855; e-mail addresses: yuehui@mail.csu.edu.cn; Wu.chonghu@cxtc.com

1359-6462/$ - see front matter © 2012 Acta Materialia Inc. Published by Elsevier Ltd. All rights reserved.
http://dx.doi.org/10.1016/j.scriptamat.2012.07.043

the vanadium oxide shell can be controlled as expected by regulating the chemical precipitation process. In addition, WC-VC core-shell powders in which the VC inhibitor clad the surface of WC powders have been fabricated through the in situ reduction and carbonization reactions of mixed $WO_3$–$V_2O_5$ and carbon powders. We demonstrate that the WC–VC core–shell structure can effectively inhibit the grain growth of finer WC particles depending on the dissolution–precipitation evolution, and finally produce cemented carbides with homogeneous and fine microstructure via an industrial sintering/hot isostatic pressing (HIP) process.

A mixed salt solution containing both tungsten and vanadium comprised ammonium tungstate ($(NH_4)_2WO_4$) and ammonium metavanadate ($NH_4VO_3$). The initial concentration of $(NH_4)_2WO_4$ solution was 0.3 mol $l^{-1}$ and the addition of $NH_4VO_3$ was controlled in accordance with the designed weight percentage of vanadium in the WC–VC–Co composite. Three kinds of samples, containing 0, 0.4 and 0.8 wt.% V, were prepared. A homogeneously mixed solution was obtained by stirring at room temperature, and then concentrated hydrochloric acid was added dropwise to the solution to form a precipitate until the pH value of solution reached 1.5, thus ensuring that all the tungsten and vanadium formed a precipitate in the solution. Subsequently, the precipitates, obtained by filtering and drying, were calcined at 500 °C in air for 4 h to form $WO_3$–$V_2O_5$ nanopowders.

The mixed powders of $WO_3$–$V_2O_5$ composite, $Co_3O_4$ and carbon according to the intended composition, with pure ethanol as the liquid medium, were milled for 50 h in a 4-planetary ball mill. Subsequently, the as-milled powder mixture was placed in a vacuum furnace at a pressure $1 \times 10^{-2}$ Pa and then heated up to 1100 °C for 2 h to conduct the in situ reduction and carbonization reactions. The composite powder was compressed into a round plate using a uniaxial pressure of 200 MPa. Sintering was carried out by sintering/HIP at 1400 °C for 60 min in Ar atmosphere with a gas pressure of 5 MPa. Alloy samples were prepared for microstructural analysis and measurement of the mechanical properties.

A D/max 2500pc X-ray diffractometer with Cu $K_\alpha$ radiation ($k = 0.154$ nm) was used to identify the phases. The microstructural observation of the powders and the densified hard metals as well as the compositional analysis of certain phases was conducted by scanning electron microscopy (SEM) using a FEI NanoSEM 230. Transmission electron microscopy (TEM) and high-resolution TEM (HRTEM) observations were carried out in JEM-2100 microscope at 200 kV. X-ray photoelectron spectroscopy (XPS) was performed on a K-Alpha spectrometer (Thermo Fisher Scientific). Hardness was measured by a Rockwell sclerometer and Vickers indentation with a load of 30 kg.

The $WO_3$–$V_2O_5$ nanopowders were prepared via an induced chemical precipitation and calcination process. Figure 1a shows typical SEM images of the $WO_3$ nanopowders, while Figure 1b gives the corresponding TEM images. The images show the presence of $WO_3$ nanopowders which are monodisperse, weakly agglomerated, and uniform and polyhedral in shape. The particle size of the $WO_3$ nanopowders is 30–80 nm. The phase and purity of the as-obtained ($WO_3$–0.8 wt.% $V_2O_5$) was determined from the XRD pattern as shown in Figure 1c. Owing to the fact that the $V_2O_5$ content is tiny, all the peaks can be indexed as orthorhombic $WO_3$ (JCPDS 20-1324) and $V_2O_5$ cannot be distinguished. The energy-dispersive X-ray spectroscopy (EDS) analysis of $WO_3$–0.8 wt.% $V_2O_5$ nanostructure indicates the presence of W, V and O elements, proving the formation of $WO_3$ and $V_2O_5$ (Fig. 1d). Subsequently, the chemical composition of all the $WO_3$ nanopowders was also investigated by EDX as shown in Table 1, with all numerical values being assigned to elemental W and O or V. The surface chemical composition of the $WO_3$ nanopowders was measured by XPS as also shown in Table 1. XPS is sensitive to the surface composition of materials and the test depths from which detectable signal intensities can be extracted are about 20 nm [12]. Owing to the fact that the addition of vanadium is too little for $WO_3$–0.4 wt.% $V_2O_5$, the disparity between the XPS and EDX values is not apparent. However, with the increase of vanadium content, the XPS value of vanadium for the $WO_3$–0.8 wt.% $V_2O_5$ is about 3 times that of the EDX value. In addition, as shown in Figure 1e, two peaks of elemental vanadium ($WO_3$–0.8 wt.% $V_2O_5$), located at 517.5 and 524.9 eV, correspond to the $V_2O_5$ binding energy of $V2p_{3/2}$ and $V2p_{1/2}$, respectively [13]. The results demonstrate that the content of element V on the powder surface is higher than the overall concentration in the powders and vanadium oxide is rich on the powder surface.

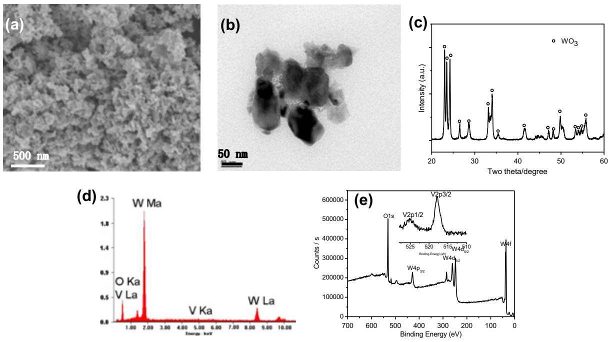

**Figure 1.** SEM (a) and TEM (b) images of $WO_3$–0.8 wt.% $V_2O_5$. XRD pattern (c), EDS spectrum (d) and XPS pattern (e) of $WO_3$–0.8 wt.% $V_2O_5$ powders.

To investigate the morphology and structure of the $WO_3$ nanopowders in depth, HRTEM of nanopowders was performed. Figure 2a shows a typical core–shell nanostructure. It can be clearly seen that the $WO_3$ core is coated with a polycrystalline $V_2O_5$ shell. From Figure 2b–d, it can be determined that the existence of the shell

**Table 1.** Experimental elemental composition obtained by EDX and XPS analysis of the $WO_3$–$V_2O_5$ powders.

| | $WO_3$–0.4 wt.% $V_2O_5$ | | | $WO_3$–0.8 wt.% $V_2O_5$ | | |
|---|---|---|---|---|---|---|
| | W (wt.%) | O (wt.%) | V (wt.%) | W (wt.%) | O (wt.%) | V (wt.%) |
| EDX | 73.16 | 26.34 | 0.50 | 63.72 | 35.20 | 0.87 |
| XPS | 78.24 | 21.15 | 0.61 | 77.24 | 20.65 | 2.11 |